

The Effects of Downcomer Diameter on an Air Entrainment of Vertical Plunging Water Jet on The Water Surface

Warjito^{1,*}, Ridho Irwansyah¹, Iqbal Yudianto¹, Leonardo Fabianto¹, Arya Amardani¹, Muhammad Nur Ilham Sukmara¹, Hasbi Mahdy Qardhawi¹

¹ Department of Mechanical Engineering, Faculty of Engineering, University of Indonesia, 16324 Depok City, East Java, Indonesia

ARTICLE INFO

Article history:

Received 18 October 2020

Received in revised form 24 February 2021

Accepted 1 March 2021

Available online 26 March 2021

Keywords:

Bubble dispersion; Downcomer; Gas entrainment rate; Vertical plunging jets; Microbubble

ABSTRACT

The difficulty in finding clean water is issued to become Indonesia's problem in 2025. Seawater processing to produce clean water for commonly used or called water desalination will be a promising solution to solve the problem of clean water scarcity. One of the seawater desalination processes is to utilize micro-bubbles generated from air entrainment. Air entrainment is a phenomenon where the surrounding air is trapped in the water and forms a bubble. Using the vertical plunging jet setup will lead to bubble formation as a result of the collision between the vertical water jet and the pond surface below it. This study determines the effect of downcomer diameter on the parameters that influence the parameter of air entrainment quality by using a vertical plunging jet configuration. Some set up tools that support research consists of pumps, nozzle, downcomer, airflow meter, anemometer, and water pond. Results of the research are in the form of qualitative data such as videos and photos, by using a high-speed camera with backlighting. The qualitative data obtained will be processed with an image processing program to acquire quantitative data. The results of the study revealed that the downcomer diameter affects the air entrainment rate. On the other hand, jet velocity affects the area of dispersion and depth of penetration.

1. Introduction

The applications of microbubble technology are appealing and expandable. One example of the use of microbubble is its application in the separation process. The separation process includes the separation of pollutants, the separation of valuable materials in mining industries, and others. Pollutant separation is a process to separate wastewater, including household wastewater, to produce a clean water source. The world's daily wastes generated are not only from large factories but households too. Roughly estimated, household waste alone contributed as much as 70% of global pollutants [1]. In the pollutant separation process, microbubbles function as a contaminant separation agent by applying hydrophobic and hydrophilic surface properties. Also, microbubbles are useful in aeration.

* Corresponding author.

E-mail address: warjito@eng.ui.ac.id

<https://doi.org/10.37934/arfmts.81.2.8997>

Fine bubbles types are divided into three types based on the size of the diameter of the bubbles formed, namely macro bubble, microbubble, and nanobubble. A microbubble is a bubble that has a diameter of 10 μm to 50 μm [2]. Microbubble can produce highly reactive free radicals without using harmful chemicals, which is regular to reduce the content of waste produced. The unique properties of microbubble make it applicable to water quality improvement, barriers reduction to mass transportation, radiology, and cardiology technology in the medical field, the process of removing microorganisms from decay factors, body washers, and also in developing shells and pearl shells [3]. The many uses of microbubble make the subject of discussion among the many applications of technology that are rife in research institutes [4], which expects favorable microbubble characteristics to be useful for the development of desalination technology.

There are many ways of producing microbubbles. One way is to take advantage of the phenomenon of entrainment of air into water. Air entrainment is a phenomenon that is responsible for mass transfer on rivers and water flow, providing oxygen and carbon dioxide transportation, using a floatation device called Jameson Cell. Jameson Cell is a tool used in the mining industry to extract mineral deposits from residual water in the form of froth, which was developed in 1985 by Graeme Jameson. It relies on air entrainment methods to create a vacuum, which leads to air suction into the downcomer. Because of the continuous waves of water jet down to the pond, air bubbles formed. Mineral sediments attached to these bubbles float to the surface, forming a layer of froth and eventually separating the sediment from water [5].

Previous studies have been able to explain the importance of physical parameters that affect the performance of the air entrainment phenomenon [3, 6]. However, some relevant phenomena have not been elucidated, including the effect of downcomer diameter on the water entrainment performance and also the role of non-dimensional numbers. Therefore, this research focused on analyzing microbubble characteristics with a downcomer diameter and the relation of air entrainment performance with non - dimensional number for better understanding.

2. Methodology

Air Entrainment research conducted by using vertical plunging jets, the experimental setup is shown in Figure 1. This experiment setup consists of a water pool, a water pump, nozzles, downcomers, an airflow meter, and a water flowmeter. There are various dimensions of nozzle and downcomer diameter were tested. Table 1 shows the operational conditions of the research. The water pump circulates the water, produces a vertical plunging water jet through the nozzle into the surface of the water pond, and generates air entrainment processes. Interaction between entrained air and water surface generates bubbles. The water flow meter and the airflow meter measure the water flow rate and the air entrainment flow rate, respectively [7, 8]. The dynamic of the generated bubble is recorded by video with a backlighting method. Minimum incoming light is needed to capture the best picture of the air entrainment. The light required only comes from the firing lamp, which is placed opposite to the camera in the pool (backlight) so that the air entrainment image obtained is as sharp as possible and clear to observe [9]. Video image then processes using image processing software to get quantitative data.

Anemometer can measure the airflow and air velocity with range measurements for airflow around 0 - 999,900 m^3/min and range for air velocity around 0.8 - 12.00 m/s [9]. The frame has a size of 1000 mm x 1400 mm x 1750 mm. Then this frame is held by a 3-inch caster wheel made of PVC. In an attempt to earn the best photography results when recording the air entrainment phenomenon, minimum incoming light is needed. The light source is limited only to the other side of the camera

direction. This configuration will create a backlight so that the air entrainment image obtained is as sharp as possible [10].

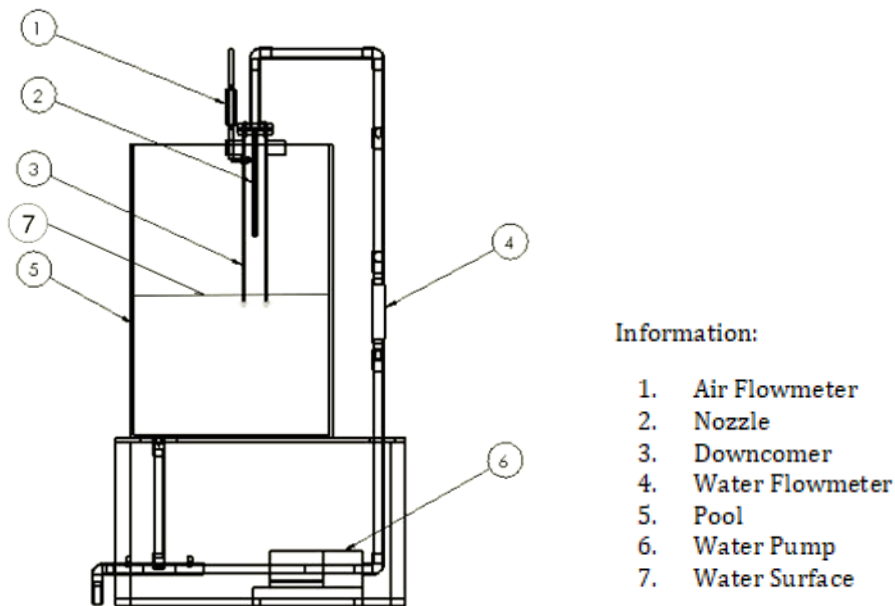


Fig. 1. Schematics of experimental tools

Table 1
 Tabulation of experimental data

No.	Independent Variable	Range	Unit
1	Nozzle Diameter	9,12,14	mm
2	Downcomer Diameter	24,34,44	mm
3	Downcomer Length	400,450,500	mm
4	Water Flowrate	10,12,14,16	Lpm

To obtain data as accurately as possible, the authors use a data processing application (image processing) named ImageJ. This software is an open-source image processing software based on Java. This software can filter images with pixels of 2048 x 2048 in just 0.1 seconds, 8-32bit in RGB color in a wide format. ImageJ offers image improvement as an optional selection, because of the need to take pictures at high speed (high-speed photo capturing).

3. Results

3.1 Microbubble Formation

The phenomenon of air entrainment was recorded and then processed to obtain qualitative data. The recorded data is then processed using the software to acquire quantitative data. The video is converted first into a series of photos that represent each recording frame before the image processing.

As illustrated in Figure 2, water jets hit the surface of the motionless water at relatively slow velocity (below the inception point). The collision forms a curve of the water-free meniscus. When the jet velocity increases, the meniscus depression also increases. If the jet speed is more than the inception speed, the air will be trapped and form bubbles and the observed entrainment. The resulting bubbles are small and follow the helicoidal path, which is around the centreline from the

direction of the jet crash. The entrained bubble moves downward, slowly decelerating. At a certain point, the speed becomes zero so that the bubbles rise to the surface of the water [6].

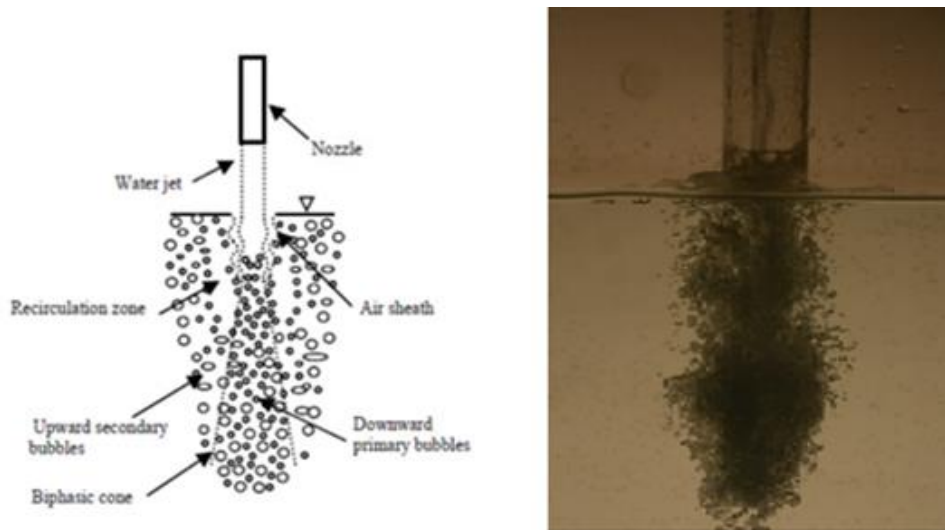


Fig. 2. Mechanism of Air Entrainment

As depicted in Figure 3, when the jet hits the surface of the water, the surface tension of the pond breaks, creating a vacuum in the form of a water cavity. Observation shows the sequence of water surface tension breaks, while the meniscus of water is carried by jets that jump from the nozzle to the pond [10]. After reaching its maximum size, the energy that comes from the rupture of the meniscus at a certain depth creates a torus bubble. The trapped air continues to move down before it splits into smaller bubbles [7].

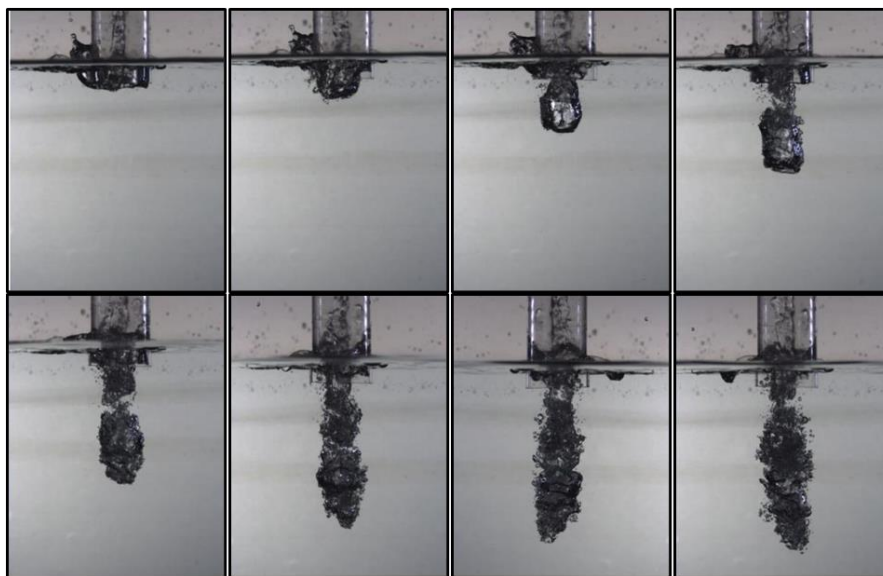


Fig. 3. Motion of Air Cavity Formation

The bubbles that formed can be evaluated and divided into two different types based on the bubble region, namely

- i. Primary Bubble, a bubble inside the conical region. The primary bubble is mostly a fine bubble that has a diameter of about 1 mm [6].

- ii. Secondary Bubble, bubbles outside the conical region on the collection of bubbles in the observation pool.

3.2 The Effect of Downcomer Diameter

From the data presented in Figure 4, there is an increase in each downcomer and discharge given. Downcomer diameter tends not to have an influence on air entrainment rate or is arguably independent [7]. The varied downcomer diameters are 24 mm, 34 mm, and 44 mm. The penetration depth chart shows the best downcomer diameter to produce the deepest penetration is 24 mm in diameter. The existing theory shows that this is true, but for the diameter with the shortest penetration depth, there is a diameter of 34 mm. The dispersion area chart shows the influence of the downcomer diameter in water discharge, which has no pattern formed on the graph displayed. The increase in water discharge shows the increase in dispersion area, although the optimum dispersion area is not at the maximum water discharge.

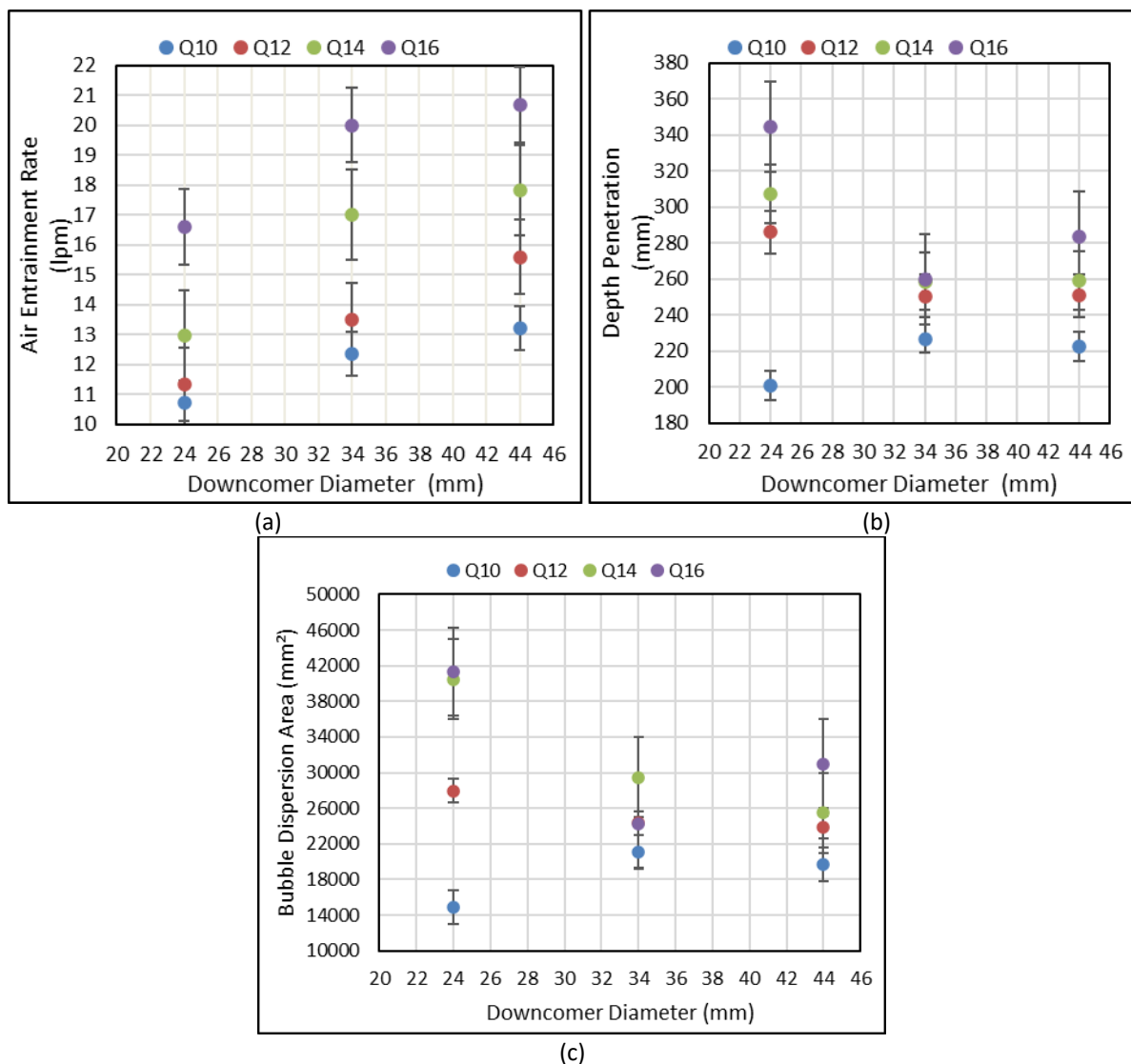


Fig. 4. Relation chart between Downcomer Diameter with (a) Air Entrainment Rate, (b) Penetration Depth, and (c) Bubble Dispersion Area

3.3 The Effect of Jet Velocity

Figure 5 shows a comparison of jet velocity with a depth of penetration at each downcomer diameter at the nozzle diameter of 9 mm. From Figure 5(a), we can see that a downcomer with a 24 mm in diameter performs the deepest penetration. The previous studies, with various diameters of the downcomer at 26 mm, 36 mm, and 46 mm, showed that a downcomer with a 36 mm in diameter performed the deepest penetration [11]. The theory put forward by Ohkawa, the downcomer diameter affects the depth of penetration. The smaller diameter of the downcomer penetrates deeper at the same jet speed [12]. The graphics presented in Figure 5(a). is in line with existing theories.

Figure 5(b) shows the relation of the nozzle diameter (D_n) and the bubble dispersion area (A_d) using a nozzle diameter of 9 mm and a downcomer length of 40 cm, the value of the bubble dispersion area almost always increases every jet speed. Only the 34 mm diameter downcomer has decreased the bubble dispersion area. In each downcomer diameter, the best value in the downcomer diameter is fluctuating between 34 mm and 24 mm. The graph at the same nozzle with the downcomer length of 45 cm and 50 cm has a different phenomenon. The value of the bubble dispersion area at a 24 mm downcomer diameter is always the highest compared to other downcomer diameters. The results obtained are in line with the graph in Figure 5(b). Of the relationship between Jet Velocity and depth of penetration, the greater the diameter of the downcomer, the smaller the bubble dispersion area produced.

Figure 5(c) depicts the value of air entrainment rate at 9 mm nozzle diameter with a Jet Velocity range from 2.62 m/s to 4.19 m/s. The most and the least air entrainment rate data is 20.68 LPM and 8.27 LPM, respectively. Following the results of the graph, at the same jet speed, the rate of air entrainment is increasing to a 34 mm downcomer. When using a 44 mm downcomer, the resulting air entrainment rate drops. The increase in the air entrainment rate is proportional to the increasing jet velocity. Variation in the height of the downcomer with 40 cm, 45 cm, and 50 cm also affects the value of the water entrainment rate. Based on the graph, the air entrainment rate decreases as the length of the downcomer increases. Compared to previous research conducted by Raka Loh Jaya, the diameter of the downcomer with the most air entrainment rate is at 26 mm [13]. Research conducted by Tasdemir downcomer diameter with the most air entrainment tends to change at every jet speed. The results of all graphs in Figure 5(c) show that the downcomer diameter tends to be independent of the air entrainment rate [14].

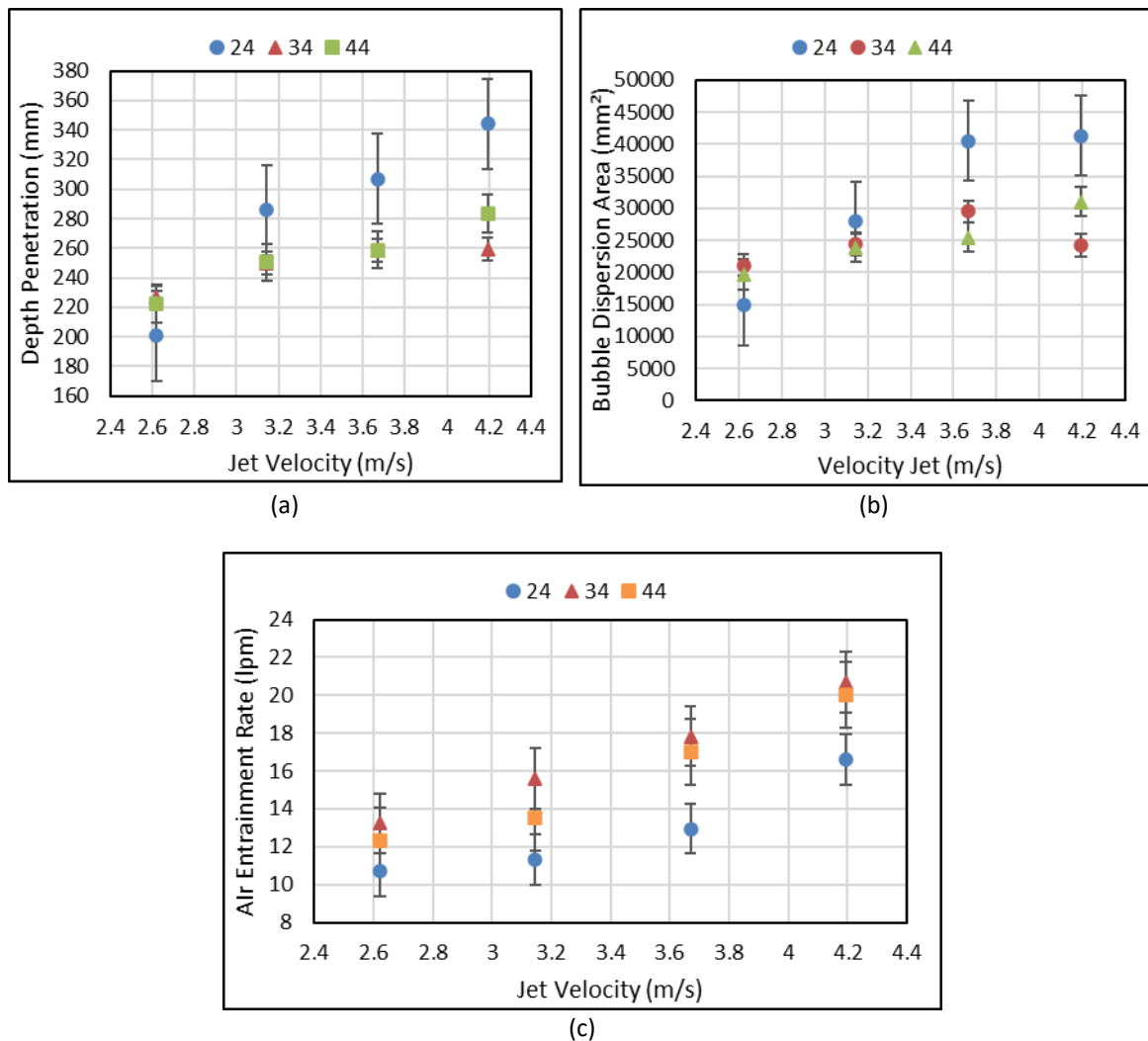


Fig. 5. Relation chart between the Jet Velocity with (a) Depth Penetration, (b) Bubble Dispersion Area, and (c) Air Entrainment Rate

3.4 Non-Dimensional Number Analysis

For a deeper understanding, an analysis of non-dimensional numbers was carried out. The non-dimensional numbers analyzed are numbers closely related to the phenomenon of bubble formation, such as Reynolds number, Weber number, and Froude number [15].

Figure 6 shows the relation of air entrainment with non-dimensional numbers with Q_g/Q_w Ratio at 24 mm downcomer diameter and 40 cm downcomer length. The symbol in the graphic, squares are 9 mm diameter nozzles, circles are 12 mm diameter nozzles, and triangles are 14 mm diameter nozzles. The density value remains constant since the working fluid is water, the Q_g/Q_w ratio on the 9 mm nozzle affects the Webber value, and the graphics depicted tend to be linear. Then on the 12 mm and 14 mm nozzles, the resulting non-dimensional numbers are not affected by the ratio.

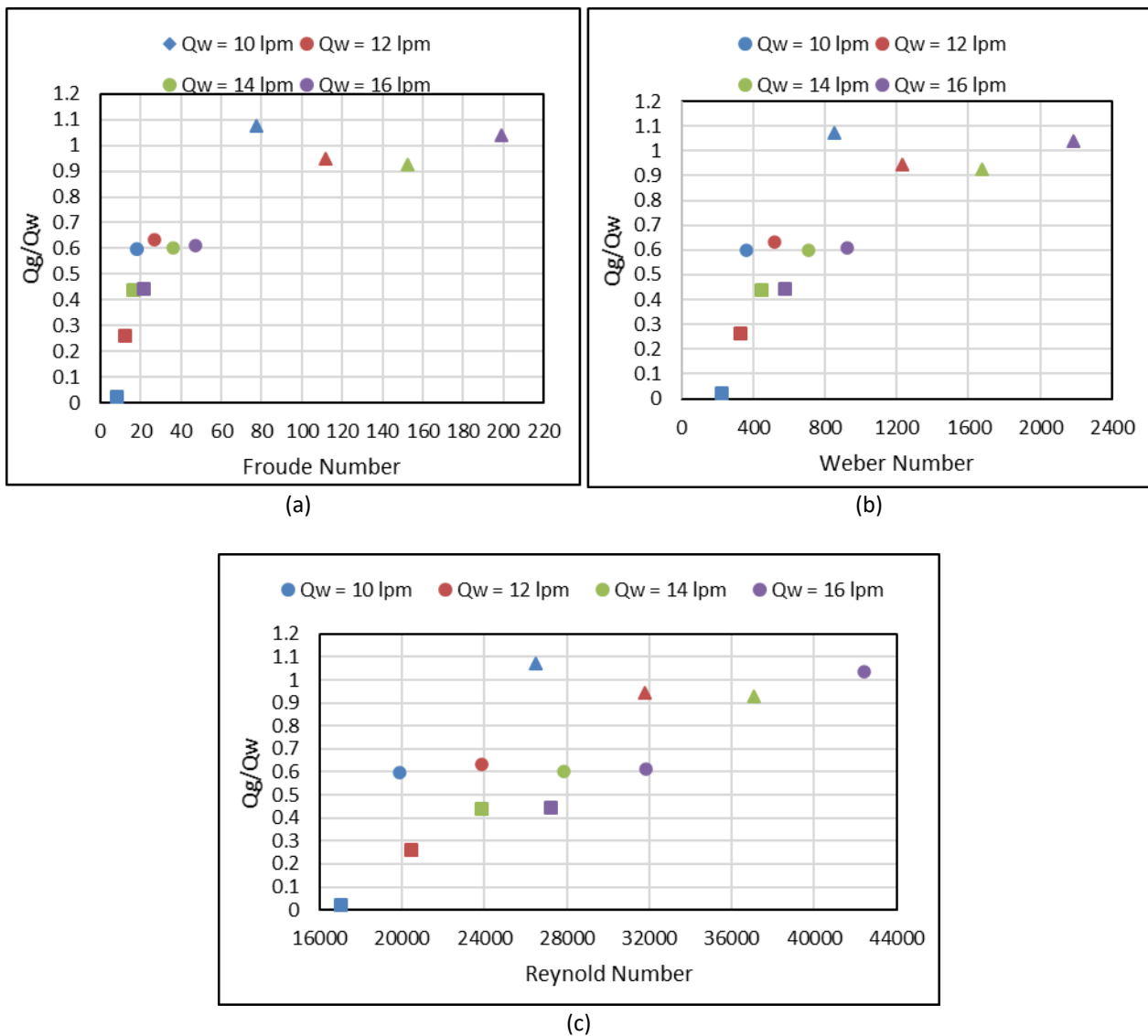


Fig. 6. Correlation between (a) Froude Number, (b) Weber Number, and (c) Reynold Number to Ratio of Water and Gas Flow Rate

4. Conclusions

This research proves that the downcomer diameter at the time of increasing water flow does not affect water entrainment and penetration depth. The downcomer diameter does not affect the bubble diffusion. However, the air discharge is directly proportional to the bubble dispersion. At the penetration depth with increasing jet velocity and downcomer diameter, it is proven that the downcomer diameter is inversely proportional to the penetration depth. The dispersion of the bubbles is directly proportional to the jet velocity. Air entrainment is independent of downcomer diameter because the optimal value of air entrainment depends on the jet velocity. Non-dimensional parameters do not show any dependency. The 9 mm nozzle size is an exceptional because it shows an effect on Weber number.

Acknowledgement

The author would like to thank Directorate of Research and Community Engagements Universitas Indonesia (DRPM UI) for funding this research through NKB-1050/UN2.RST/HKP.05.00/2020, the International Publication Index (PUTI) 2020 scheme.

References

- [1] Tamura, Iwao, Ikuo Uehara, and Kazuyoshi Adachi. "Developing a micro-bubble generator and practical system for purifying contaminated water." *Stud. Sci. Technol* 3, no. 1 (2014): 87-90.
- [2] Agarwal, Ashutosh, Wun Jern Ng, and Yu Liu. "Principle and applications of microbubble and nanobubble technology for water treatment." *Chemosphere* 84, no. 9 (2011): 1175-1180. <https://doi.org/10.1016/j.chemosphere.2011.05.054>
- [3] Jaya, Raka Loh. "The effect of diameter downcomer in air entrainment process from vertical plunging water jet with downcomer." In *IOP Conference Series: Materials Science and Engineering*, vol. 539, no. 1, p. 012024. IOP Publishing, 2019. <https://doi.org/10.1088/1757-899X/539/1/012024>
- [4] Laksana, M. "Micro-bubble generator dengan metode spherical ball dalam pipa beraliran." *Skripsi, Universitas Indonesia, Jakarta* (2008).
- [5] Clayton, R., G. J. Jameson, and E. V. Manlapig. "The development and application of the Jameson cell." *Minerals Engineering* 4, no. 7-11 (1991): 925-933. [https://doi.org/10.1016/0892-6875\(91\)90074-6](https://doi.org/10.1016/0892-6875(91)90074-6)
- [6] Saadabadi, M. Saeed Ebrahimi, Ehsan Yousefi, Kiyan Khaloozadeh, and Hamid Khaloozadeh. "Airflow estimation of a laboratory Anemometer via fisher statistical technique." In *2017 10th International Symposium on Advanced Topics in Electrical Engineering (ATEE)*, pp. 818-822. IEEE, 2017. <https://doi.org/10.1109/ATEE.2017.7905173>
- [7] Takahashi, Masayoshi, Kaneo Chiba, and Pan Li. "Free-radical generation from collapsing microbubbles in the absence of a dynamic stimulus." *The Journal of Physical Chemistry B* 111, no. 6 (2007): 1343-1347. <https://doi.org/10.1021/jp0669254>
- [8] Deane, Grant B., and M. Dale Stokes. "Air entrainment processes and bubble size distributions in the surf zone." *Journal of Physical Oceanography* 29, no. 7 (1999): 1393-1403. [https://doi.org/10.1175/1520-0485\(1999\)029<1393:AEPABS>2.0.CO;2](https://doi.org/10.1175/1520-0485(1999)029<1393:AEPABS>2.0.CO;2)
- [9] Garcia, Patxi, Yusuke Mori, and Yusaku Kyojuka. "Improvement of Water Quality by Microbubble Generation in Hakata Bay: Experiment and Simulation." In *Conference proceedings, the Japan Society of Naval Architects and Ocean Engineers* 19 (2014): 143-146.
- [10] Kiger, Kenneth T., and James H. Duncan. "Air-entrainment mechanisms in plunging jets and breaking waves." *Annual Review of Fluid Mechanics* 44 (2012): 563-596. <https://doi.org/10.1146/annurev-fluid-122109-160724>
- [11] R. L. Jaya, "Pengaruh Diameter Downcomer pada Proses Air Entrainment dari Vertical Plunging Water Jet dengan Downcomer." 2018.
- [12] Ohkawa, A., D. Kusabiraki, Y. Kawai, N. Sakai, and K. Endoh. "Some flow characteristics of a vertical liquid jet system having downcomers." *Chemical Engineering Science* 41, no. 9 (1986): 2347-2361. [https://doi.org/10.1016/0009-2509\(86\)85085-0](https://doi.org/10.1016/0009-2509(86)85085-0)
- [13] Biń, Andrzej K. *Gas entrainment by plunging liquid jets*. VDI-Verlag, 1988. [https://doi.org/10.1016/0009-2509\(93\)81019-R](https://doi.org/10.1016/0009-2509(93)81019-R)
- [14] Taşdemir, T., B. Öteyaka, and A. Taşdemir. "Air entrainment rate and holdup in the Jameson cell." *Minerals Engineering* 20, no. 8 (2007): 761-765. <https://doi.org/10.1016/j.mineng.2007.02.008>
- [15] Hristov, Jordan. "Benchmarking of the construct of dimensionless correlations regarding batch bubble columns with suspended solids: Performance of the Pressure Transform Approach." *arXiv preprint arXiv:1012.6004* (2010).